공학석사 학위논문

Size Characterization of Ultrasmall Silver Nanoparticles Using MALDI-TOF Mass Spectrometry

MALDI-TOF를 이용한

극소 은 나노입자 크기 분석

2015년 2월

서울대학교 대학원

화학생물공학부

장 호 근

Size characterization of Ultrasmall Silver Nanoparticles Using MALDI-TOF Mass Spectrometry

지도 교수 현 택 환

이 논문을 공학석사 학위논문으로 제출함

2014년 12월

서울대학교 대학원

화학생물공학부

장 호 근

장호근의 공학석사 학위논문을 인준함

2014년 12월

위 원 장 ______________________ (인)

부위원장 ______________________ (인)

위　　원 ______________________ (인)

Abstract

Size characterization of Ultrasmall Silver Nanoparticles Using MALDI-TOF Mass Spectrometry

Hogeun Chang

School of Chemical and Biological Engineering

The Graduate School

Seoul National University

We present a rapid and reliable method to determine the sizes and size distributions of silver nanoparticles smaller than 5 nm using matrix-assisted laser desorption & ionization-time-of-flight (MALDI-TOF) mass spectrometry (MS). The MS data could be converted to size information using a simple equation derived by Cardano's formula.

Calculated coefficients of size-to-mass equation were different, but the differences among the data set were negligible. Furthermore, size-to-mass

equation for anisotropic particles were derived by similar process done for spherical particles. This suggests MALDI-TOF MS could be used not only for characterizing size properties, but also for characterizing shapes and sizes with high accuracy. This shows MALDI-TOF MS as useful technique in nanotechnology.

Keywords: Ultrasmall nanoparticle, silver nanoparticle, MALDI-TOF, Mass spectrometry.

Student Number: 2013-20993

Contents

List of Tables

List of Figures

1. Introduction

1.1 Ultrasmall nanoparticles

Ultrasmall nanoparticles have recently been the interesting subject of research owing to the unique physical and chemical properties manifest in the particles as their size approaches a molecular dispersion.[1–3] Among the ultrasmall nanoparticles, ultrasmall silver nanoparticles were actively researched because of their unique optical and magnetic properties. Although silver is diamagnetic in the bulk state, ultrasmall silver nanoparticles were found to be ferromagnetic.[4] When silver nanoparticles have small size as a few nanometers, the electronic energy levels become quantized, and the particles emit luminescence.[5] This luminescence has been used as an in vitro optical imaging probe.[6] The magnetic and optical properties of ultrasmall silver nanoparticles are highly size dependent and are derived from the surface of the particle. As particles become smaller in size, the total surface area increases while the core size decreases such that small enough particles may have no core atoms at all.[7] According to these aspects, there are two main procedures to control the functional properties of these particles, first controlling the size of the particle during synthesis, and second measuring the size distribution accurately. With regard to the latter, microscopic techniques such as transmission electron microscopy (TEM) are the standard for measuring the size of nanoparticles. However, these measurements do not provide accurate estimates of the polydispersity of the total population considering only a very small fraction of particles are observed and measured. Moreover, poor contrast and a tendency for ablation in the electron beam makes the quantification of the total surface area of ultrasmall nanoparticles very difficult.[8] X-ray diffraction (XRD) has been used as an alternative to determine the size of nanoparticles according to the Scherrer equation, but this methods also has inherent inaccuracies because the peak width is also affected by shape and crystallinity. Also, dynamic light scattering (DLS) is a probable method for measuring size of nanoparticles, however the low intensity of scattered light induced by ultrasmall particles makes it difficult to characterize these nanoparticles. Recently, mass spectrometry (MS) has been garnering attention in the quantification of particle size.[9–12]

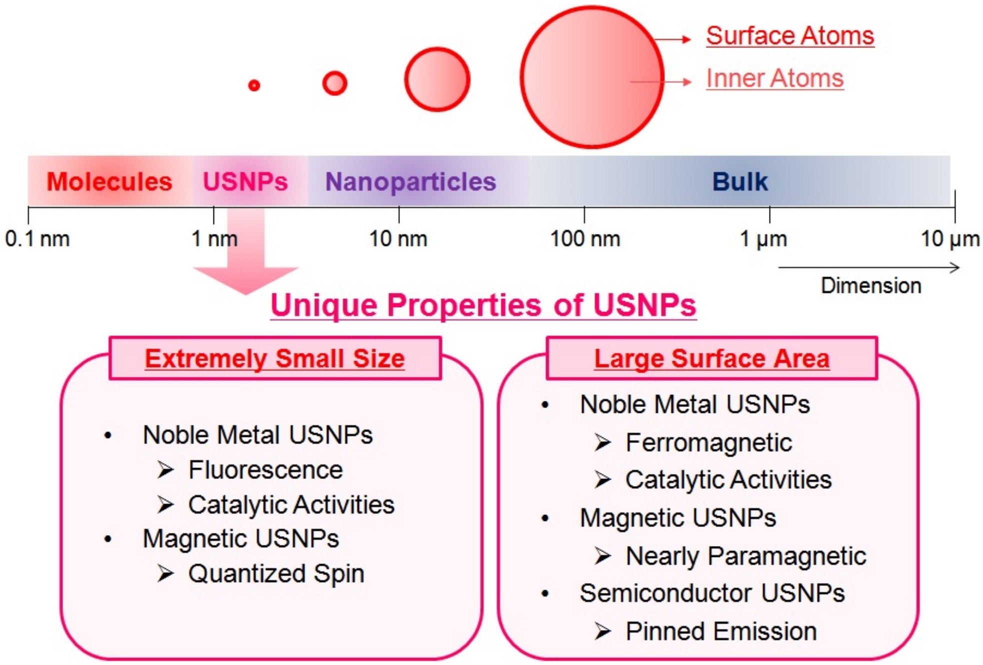

Figure 1. Schematic diagram juxtaposing the difference in the sizes of particles and their resultant properties. (from Ref. [14], Kim, B. H.; Hackett, M. J.; Park, J.; Hyeon, T. *Chem. Mater.* **2014**, 26, 59)

1.2 Mass spectrometry

MS has long been one of the most important characterization tools in the fields of chemistry and biology. The spectra are obtained following the ionization of the sample and subsequent sorting based on the mass to charge ratio in magnetic and electric fields. If nanoparticles can be stable under the ionization conditions, the calculated mass provided by MS could then be used to estimate the size of nanoparticles. There are several methods of ionization, the first of which involves subjecting the sample to a large potential causing it to disaggregate (electrospray ionization, ESI). Desorption and ionization process can be assisted by ablation with a high energy laser (matrix assisted laser desorption/ionization, MALDI) or a salvo of inert gases (fast atom bombardment, FAB). For the purpose of quantifying nanoparticles, the particle must remain intact during ionization. Thus to reduce sample fragmentation, the more mild conditions of MALDI have been extensively used. Particles ionized by MALDI were analyzed by a time of flight (TOF) analyzer which correlates the time it takes from ionization to detection with the mass of the ion. Thus MALDI-TOF MS could be employed to characterize ultrasmall nanoparticles as it can quantitate many particles at a time leading to a much better estimate of dispersity. The size range of particles that can be quantified by TOF is very large and highly sensitive. Whetten et al. first reported the mass of thiol-capped gold nanoparticles could be measured by MS.[9] ZnS nanoparticles stabilized by n-hexadecylamine were analyzed by MS and the results compared to TEM and UV spectroscopy.[10] Moreover, Kumara et al. use both ESI and MALDI-TOF MS for analyzing gold nanoclusters stabilized by phenylethanethiol. Not only the number of gold atom, but also that of surfactant was calculated.[15-16]

Recently, Kim et al. obtained the MALDI-TOF mass spectra of 70 batches of ultrasmall iron oxide nanoparticles and provided a size-to-mass conversion equation. This equation is very accurate because it was derived by considering both the mass of the core and that of the ligand.[12] In spite of the recent progress on the measurement of nanoparticles by MS, only a few types of nanoparticles (Au, ZnS, iron oxide) have been investigated by MALDI-TOF MS. This paper will focus on the mass characterization of ultrasmall silver nanoparticles by MALDI-TOF MS and the subsequent conversion of the mass data to size distributions.

2. Experimental Section

2.1 Synthesis of ultrasmall silver nanoparticles

Ultrasmall silver nanoparticles were prepared by the previously reported method.[13] 0.17g of silver nitrate (1.0 mmol, Strem Chemical) was added to 0.5 mL of oleylamine (Acros Organics) and 4.5 mL of oleic acid (Sigma-Aldrich Inc.). The mixture was degassed at 70 °C for 90 min under vacuum and the reaction vessel was purged with argon. For the synthesis of 1.8 nm-sized nanoparticles, the solution was heated to 180 °C at a heating rate of 10 °C/min and maintained for 2 min. For 3.7 nm-sized nanoparticles, the heating rate was set to 1 °C/min and the reaction was stopped when the temperature just reached 180 °C. After the reaction, the reaction vessel was cooled to room temperature and washed with mixture of toluene and ethanol. The ratio of toluene and ethanol was 1:5. After washing process, nanoparticles were dispersed in chloroform.

2.2 Characterization

MALDI-TOF MS was performed on a Voyager-DETM STR Biospectrometry Workstation (Applied Biosystems). Nanoparticles dispersed in chloroform were mixed with 9-nitroanthracene dissolved in chloroform (Sigma-Aldrich Inc.) in a weight ratio of 1:1 and spotted onto a target plate. The mass spectra were obtained with the 40 ~ 50% of the laser’s full power. All of the mass spectra were smoothed with a simple average of 100 data points. TEM images were taken with a JEOL-2010 electron microscope and TGA data were collected with a Q-5000 IR (TA Instrument).

3. Results & Discussion

3.1 Characterization of synthesized ultrasmall silver nanoparticle

The sizes of silver nanoparticle populations were measured from TEM images. The TEM images are presented in Figure 2 and the corresponding particle sizes were measured as 1.3, 1.6, 1.8, 1.8, 2.4, and 3.7 nm, respectively. 9-nitroanthracene was selected as the ionization matrix because the ultrasmall silver nanoparticles are easily dispersed in hydrophobic media. Furthermore, the matrix well absorbs the wavelength of the laser source (N_2 laser; 377 nm) and it interacts weakly with the surface of silver nanoparticles. Using 9-nitroanthracene as a matrix, MALDI-TOF mass spectra of ultrasmall silver nanoparticles were obtained. For 1.8nm silver nanoparticles, the mass obtained by MALDI-TOF was 41.9 kDa. (Figure 2c).

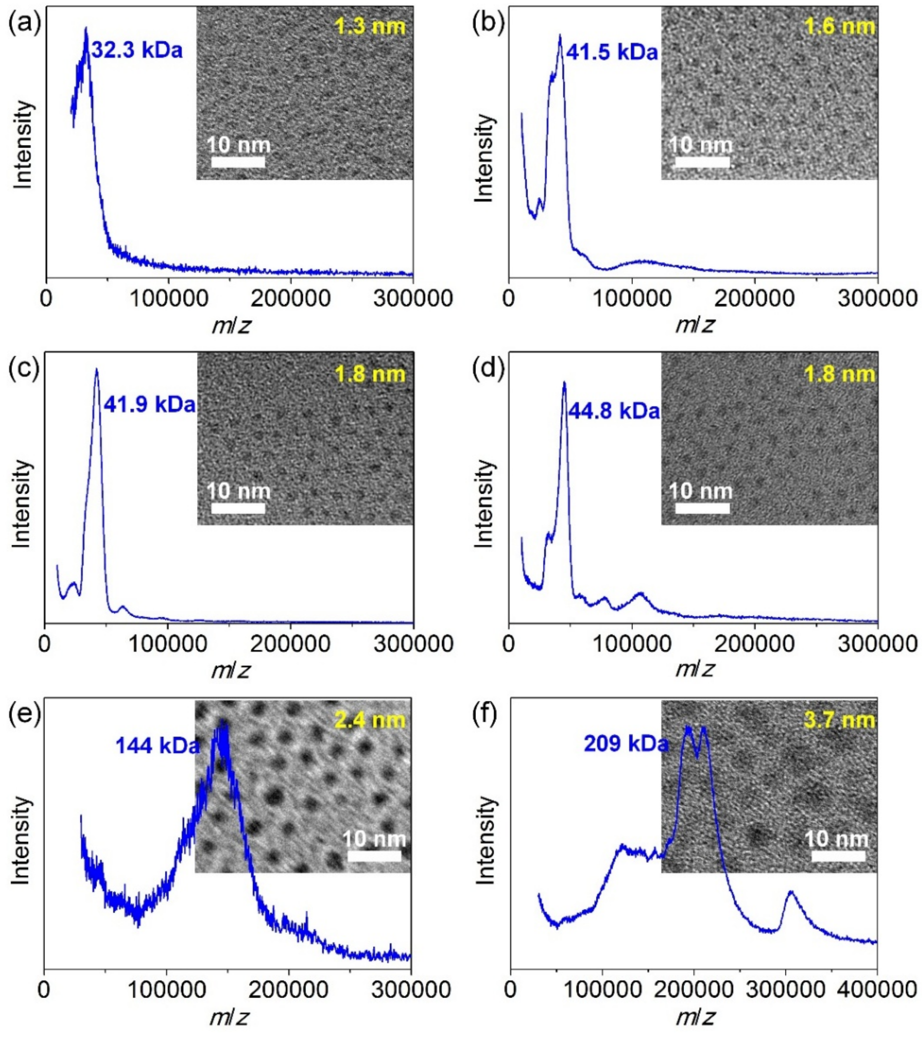

Figure 2. MALDI-TOF mass spectra and corresponding TEM images for various sized ultrasmall silver nanoparticles.

3.2 Size-to-mass correlation function for spherical particles

The correlation function, which converts the mass of a particle into a diameter, was derived from a simple assumption. Because nanoparticles consist of an inorganic core as well as organic ligands, the total mass of the particle can be described as the sum of these masses (i.e. $\boldsymbol{M} = \boldsymbol{M}_{core} + \boldsymbol{M}_{ligand}$). Assuming the nanoparticle is spherical in shape, the mass of the particle can be expressed as the third order equation with respect to the diameter as described in Eq. (1):

$$\boldsymbol{M} = \rho N_A \cdot \frac{\pi \boldsymbol{D}^3}{6} + \sigma \cdot \pi \boldsymbol{D}^2 = a\boldsymbol{D}^3 + b\boldsymbol{D}^2 \quad (1)$$

In this equation, ρ is the density of the core (1.05×10^{-20} g/nm^3 for silver), N_A is Avogadro's number (6.02×10^{23} mol^{-1} = Da/g), D is diameter of a nanoparticle (nm), σ is surface density of ligand (Da/nm^2). All of the coefficients are known except σ. The surface density can be acquired from the core weight fraction (f) which can be measured by TGA. The core fraction is represented by the function of σ as follows in Eq. (2):

$$f = \frac{\boldsymbol{M}_{\text{core}}}{\boldsymbol{M}} = \frac{\rho N_{\text{A}} \cdot \frac{\pi \boldsymbol{D}^3}{6}}{\rho N_{\text{A}} \cdot \frac{\pi \boldsymbol{D}^3}{6} + \sigma \cdot \pi \boldsymbol{D}^2} \qquad (2)$$

Eq. (2) can be rearranged to Eq. (3) as follows:

$$\sigma = \frac{\rho N_A \boldsymbol{D}(1 - f)}{6f} \qquad (3)$$

The σ value was then calculated from the TGA (f) and TEM ($\boldsymbol{D}$) data. The surface ligand density was nearly constant and average surface ligand density was 3.12×10^3 Da/nm^2 (Table 1). By substituting the σ value into Eq. (2), the third (a) and second (b) order coefficients of $\boldsymbol{D}$ were obtained: $a = 3.31 \times 10^3$ Da/nm^3, $b = 9.82 \times 10^3$ Da/nm^2. The size could then be represented as a function of mass by rearranging Eq. (1) using Cardano's method as follows in Eq. (4)

$$\boldsymbol{D} = \alpha + \sqrt[3]{\alpha^3 + \beta \boldsymbol{M} + \sqrt{2\alpha^3 \beta \boldsymbol{M} + \beta^2 \boldsymbol{M}^2}} + \sqrt[3]{\alpha^3 + \beta \boldsymbol{M} - \sqrt{2\alpha^3 \beta \boldsymbol{M} + \beta^2 \boldsymbol{M}^2}} \qquad (4)$$

where $\alpha = -2\sigma/\rho N_A \approx -0.990$ (nm) and $\beta = 3/\rho N_A \pi \approx 1.51 \times 10^{-4}$ (nm^3/Da). A plot of Eq. (4) for silver particles is presented in Figure 4. Using Eq. (4), the particle size can be easily estimated from mass data obtained with MALDI-TOF MS. The size of ultrasmall silver nanoparticles having a 41.9 kDa mass is 1.66 nm, and the size of a 44.8 kDa nanoparticle is 1.70 nm which correlates well with the size estimated from TEM (1.8 nm each). The 2.9 kDa difference from the mass data turns out to be 0.04 nm, demonstrating the high sensitivity of MS. This sensitivity is derived from the third order relationship between mass and diameter.

Although the surface ligand density was assumed to be constant, it is known to be affected by the microenvironment at the interface of the surface and the solvent. To investigate the effects of variable surface ligand density on Eq. (4), the maximum and minimum values of surface ligand density (Table 1) were applied to the calculation in the case of ultrasmall silver nanoparticles. The observed surface ligand densities ranged from 2.78×10^3 Da/nm^2 to 3.37×10^3 Da/nm^2, thus the corresponding *b* coefficients in Eq. (4) would range from 8.73×10^3 Da/nm^2 to 1.06×10^4 Da/nm^2, respectively (Table 2). The correlation curves calculated with these coefficients are depicted in Figure 4. By employing the range of the surface ligand density, the mass of the particles may be used to calculate a size range. For example, a 41.9 kDa nanoparticle would have an estimated maximum diameter of 1.71 nm ($\sigma = 2.72 \times 10^3$ Da/nm^2) and a minimum diameter of 1.62 nm ($\sigma = 3.22 \times 10^3$ Da/nm^2). This predicted range is smaller than 1 Å (0.1 nm), suggesting minor changes in the surface ligand density can be ignored when calculating the particle size by MALDI-TOF MS.

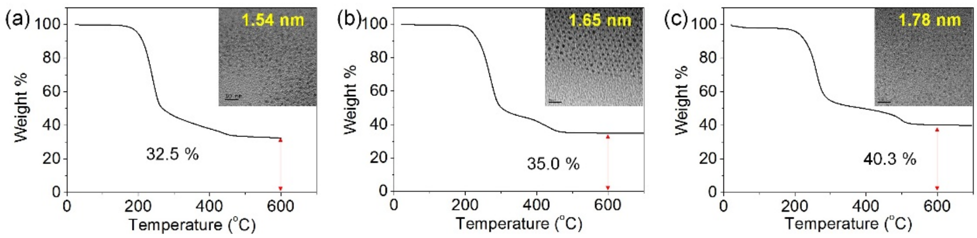

Figure 3. Thermogravimetric analysis (TGA) data and corresponding transmission electron microscopy (TEM) images of ultrasmall silver nanoparticles.

	Size(nm)	**Core Fraction**	**Ligand Density (10^3 Da/nm^2)**
Figure 3a	1.54	0.325	3.37
Figure 3b	1.65	0.35	3.23
Figure 3c	1.78	0.403	2.78

Table 1. Surface ligand density derived from TEM images and corresponding TGA data of Figure 3.

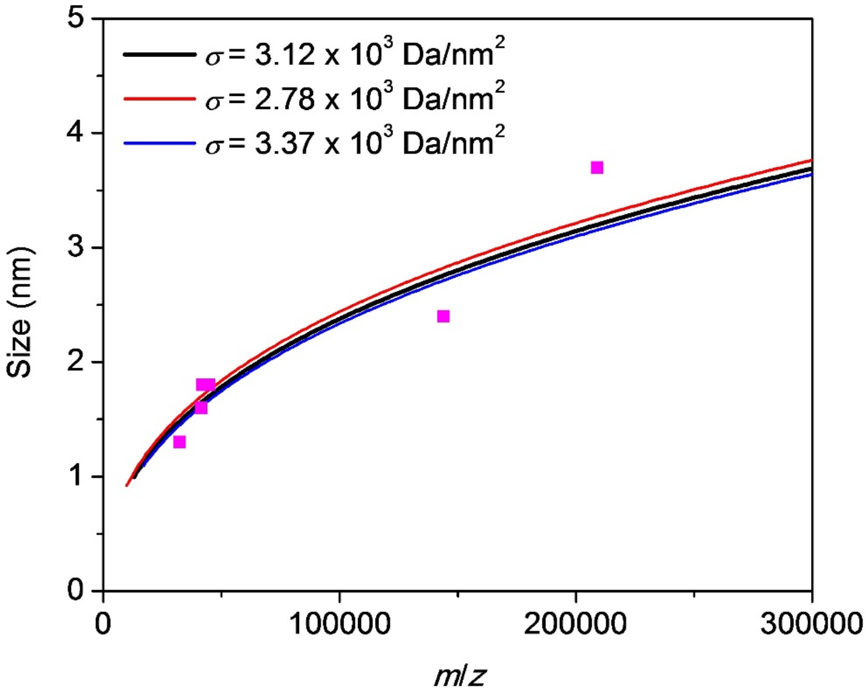

Figure 4. Solid curves indicate the size-to-mass correlation equation in different surface ligand density (black: 3.12; red: 2.78; blue: 3.37×10^3 Da/nm^2) from Eq. (4). The position of each pink dot indicates the mass peak position (x-axis) and the mean diameter measured from TEM images in Figure 2.

3.3 Size-to-mass correlation function for anisotropic particles

The size-to-mass correlation equation (Eq. (4)) can also be applied to non-spherical nanoparticles. However, it is very difficult to synthesize anisotropic ultrasmall nanoparticles so the particles were modeled to compare them with the spherical particles. We modeled cube- or octahedron-shaped nanoparticles, because silver particles have a cubic crystal lattice (Figure 5a, b). According to Figure 5a, the total mass (sum of core and ligand masses) of cubic nanoparticles can be described as follows in Eq. (5):

$$\boldsymbol{M} = \rho N_{\mathrm{A}}(2\boldsymbol{L})^3 + \sigma \cdot 6 \cdot (2\boldsymbol{L})^2 \qquad (5)$$

In this equation, $\boldsymbol{L}$ is half of the edge length (intercept of cube, see Figure 5a). It is necessary to convert the edge length to an average diameter in order to compare the equation with the spherical particles. To do this, the root mean square radius was substituted for the mean radius because the calculation of the average diameter of cube is extremely arduous. The root mean square radius of the top face of cube was also calculated (blue color in Figure 5a).

$$\sqrt{\langle \boldsymbol{r} \rangle^2} = \sqrt{\frac{\int_{-L}^{L}\int_{-L}^{L} r^2 dxdy}{\int_{-L}^{L}\int_{-L}^{L} dxdy}} = \sqrt{\frac{\int_{-L}^{L}\int_{-L}^{L}\left(\sqrt{x^2+y^2+\boldsymbol{L}^2}\right)^2 dxdy}{\int_{-L}^{L}\int_{-L}^{L} dxdy}} = \sqrt{\frac{5}{3}}\boldsymbol{L} \quad (6)$$

$$\boldsymbol{D} \approx 2\sqrt{\langle \boldsymbol{r} \rangle^2} = 2\sqrt{\frac{5}{3}}\boldsymbol{L} \quad (7)$$

The result can be regarded as the root mean square radius of the cube considering the six faces of cube are equivalent. Substituting Eq. (7) into Eq. (5), the total mass of the nanoparticles is expressed as a third order formula with respect to the diameter as follows in Eq. (8):

$$\boldsymbol{M} = \left(\frac{3}{5}\right)^{\frac{3}{2}} \rho N_A \boldsymbol{D}^3 + \frac{18}{5}\sigma \boldsymbol{D}^2 = a\boldsymbol{D}^3 + b\boldsymbol{D}^2 \quad (8)$$

Eq. (8) can be rearranged using Cardano's method resulting in the cubic-equivalent of Eq. (4) with coefficient values of $\alpha = -2\sqrt{5}\sigma/\sqrt{3}\rho N_A$ and $\beta = 5\sqrt{5}/6\sqrt{3}\rho N_A$. For ultrasmall cubic silver nanoparticles, the coefficients α and

β are estimated to be -1.28 (nm) and 1.70 × 10^{-4} (nm^3/Da), respectively (Table 2).

The size-to-mass conversion equation for octahedral nanoparticles was similarly derived for cubic particles. The total mass (***M***) is denoted as follows in Eq. (9):

$$\boldsymbol{M} = \rho N_A \cdot \frac{4}{3}\boldsymbol{h}^3 + \sigma \cdot 8 \cdot \frac{\sqrt{3}}{2}\boldsymbol{h}^2 \quad (9)$$

In this equation, ***h*** is half the axis length (intercept of Figure 5b). The root mean square radius can be calculated by using one face of the octahedron.

$$\sqrt{\langle \boldsymbol{r} \rangle^2} = \sqrt{\frac{\int_0^{\boldsymbol{h}}\int_0^{\boldsymbol{h}-y} r^2 dxdy}{\int_0^{\boldsymbol{h}}\int_0^{\boldsymbol{h}-y} dxdy}} = \sqrt{\frac{\int_0^{\boldsymbol{h}}\int_0^{\boldsymbol{h}-y} \left(\sqrt{x^2+y^2+(\boldsymbol{h}-x-y)^2}\right)^2 dxdy}{\int_0^{\boldsymbol{h}}\int_0^{\boldsymbol{h}-y} dxdy}} \quad (10)$$

$$\boldsymbol{D} \approx 2\sqrt{\langle \boldsymbol{r} \rangle^2} = \sqrt{2}\boldsymbol{h} \quad (11)$$

The result can be regarded as the total root mean square radius as all eight faces of octahedron are equivalent. Substituting Eq. (11) into Eq. (9), the total mass of the nanoparticles can be expressed as a third order formula with respect to the diameter as follows in Eq. (12):

$$\boldsymbol{M} = \frac{\sqrt{2}}{3}\rho N_A \boldsymbol{D}^3 + 2\sqrt{3}\sigma \boldsymbol{D}^2 = a\boldsymbol{D}^3 + b\boldsymbol{D}^2 \quad (12)$$

After rearrangement of Eq. (12) into the octahedral-equivalent of Eq. (4), coefficient values of $\alpha = -\sqrt{6}\sigma/\rho N_A$ and $\beta = 3/2\sqrt{2}\rho N_A$ were obtained. For octahedral silver nanoparticles, the coefficients α and β are estimated to be -1.21 (nm) and 1.68×10^{-4} (nm^3/Da), respectively (Table 2).

The solution of the size-to-mass conversion equations for cubic, octahedral and spherical particles are plotted in Figure 5c. Although the equations were derived using the root mean square radius, the resulting equations for the cubic and octahedral particles are very similar to the spherical particles. Consequently, it is expected the size-to-mass conversion equation can be adopted not only for the analysis of spherical nanoparticles, but also for the analysis of cubic or octahedral nanoparticles.

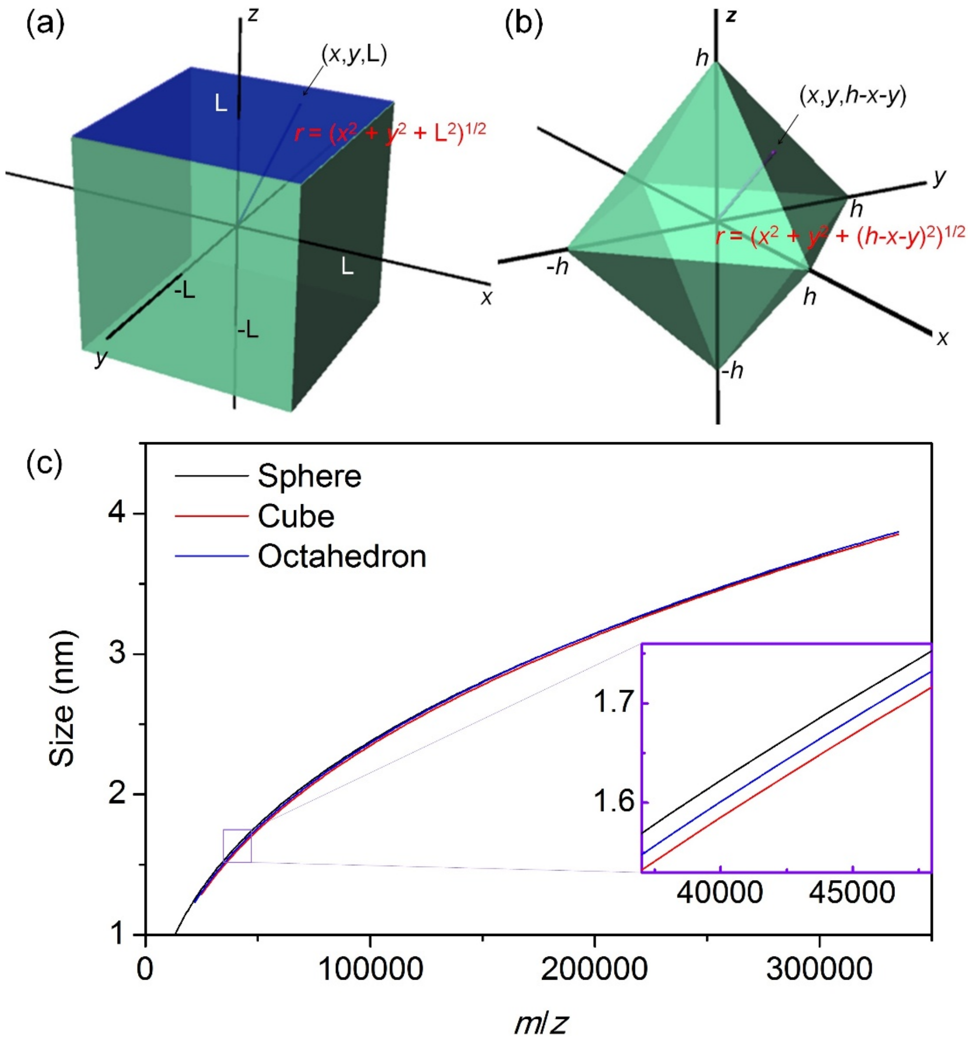

Figure 5. (a) Cube and (b) octahedron models in the rectangular coordinates. (c) Size-to-mass estimation curves for spherical, cubic, and octahedral silver nanoparticles.

Graph	***Core density*** ***(10^{-20} g/nm^3)***	***Surface density*** ***(10^3 Da/nm^2)***	***shape***	***a*** ***(10^3 Da/nm^3)***	***b*** ***(10^3 Da/nm^2)***	***α*** ***(nm)***	***β*** ***(10^{-4} nm^3/Da)***	***Calculated size at 41.9 kDa*** ***(nm)***	***Calculated size at 100 kDa*** ***(nm)***
Fig.3,5	1.05	3.13	Sphere	3.31	9.82	-0.990	1.51	1.66	2.38
Fig.3	1.05	**2.78**	Sphere	3.31	8.73	-0.879	1.51	1.71	2.44
Fig.3	1.05	**3.37**	Sphere	3.31	10.6	-1.07	1.51	1.62	2.33
Fig.5	1.05	3.13	**Cube**	2.94	11.3	-1.28	1.70	1.62	2.34
Fig.5	1.05	3.13	**Octahedron**	2.98	10.8	-1.21	1.68	1.63	2.37

Table 2. Coefficient of Eq. (4) in different surface density and shape.

4. Conclusion

In conclusion, MALDI-TOF mass spectra of spherical silver nanoparticles with 9-nitroanthracene matrix were successfully used to estimate the corresponding particle sizes. The mass data were converted into a size distribution using a derived size-to-mass equation which correlated well with the sizes measured by TEM.

Although the coefficients of the size-to-mass equation are not constant in ultrasmall nanoparticles, the differences shown by the results are negligible. Furthermore, this equation should be compatible not only with spherical particles but also with anisotropic particles such as cubic- or octahedral-shaped particles. This suggests MALDI-TOF MS could be used as a generic methodology for estimating the particle size distribution of nanoparticles with various shapes and sizes with high accuracy making it a very valuable and versatile technique in nanotechnology.

5. References

[1] Gatteschi, D.; Fittipaldi, M.; Sangregorio, C.; Sorace, L. *Angew. Chem., Int. Ed.* **2012**, 51, 4792.

[2] Harrell, S. M.; McBride, J. R.; Rosenthal, S. J. *Chem. Mater.* **2013**, 25, 1199.

[3] Kim, B. H.; Lee, N.; Kim, H.; An, K.; Park, Y. I.; Choi, Y. S.; Shin, K.; Lee, Y.; Kwon, S. G.; Na, H. B.; Park, J.-G.; Ahn, T.-Y.; Kim, Y.-W.; Moon, W. K.; Choi, S. H.; Hyeon, T. *J. Am. Chem. Soc.* **2011**, 133, 12624.

[4] Garitaonandia, J. S.; Insausti, M.; Goikolea, E.; Suzuki, M.; Cashion, J. D.; Kawamura, N.; Ohsawa, H.; Muro, I. G.; Suzuki, K.; Plazaola, F.; Rojo, T. *Nano Lett.* **2008**, 8, 661.

[5] Yuan, X.; Luo, Z.; Yu, Y.; Yao, Q.; Xie, J. *Chem. Asian J.* **2013**, 8, 858.

[6] Yu, J.; Patel, S. A.; Dickson, R. M. *Angew. Chem., Int. Ed.* **2007**, 46, 2028.

[7] Nützenadel, C.; Züttel, A.; Chartouni, D.; Schmid, G.; Schlapbach, L. *Eur. Phys. J. D* **2000**, 8, 245.

[8] Wilcoxon, J. P.; Martin, J. E.; Provencio, P. *Langmuir* **2000**, 16, 9912.

[9] Whetten, R. L.; Khoury, J. T.; Alvarez, M. M.; Murthy, S.; Vezmar, I.; Wang, Z. L.; Stephens, P. W.; Cleveland, C. L.; Luedtke, W. D.; Landman, U. *Adv. Mater.* **1996**, 8, 428.

[10] Khitrov, G. A.; Strouse, G. F. *J. Am. Chem. Soc.* **2003**, 125, 10465.

[11] Kasuya, A.; Sivamohan, R.; Barnakov, Y. A.; Dmitruk, I. G.; Nirasawa, T.; Romanyuk, V. R.; Kumar, V.; Mamykin, S. V.; Tohji, K.; Jeyadevan, B.; Shinoda, K.; Kudo, T.; Terasaki, O.; Liu, Z.; Belosludov, R. V.; Sundararajan, V.; Kawazoe, Y. *Nat. Mater.* **2004**, 3, 99.

[12] Kim, B. H.; Shin, K.; Kwon, S. G.; Jang, Y.; Lee, H.-S.; Lee, H.; Jun, S. W.; Lee, J.; Han, S. Y.; Yim, Y.-H.; Kim, D.-H.; Hyeon, T. *J. Am. Chem. Soc.* **2013**, 135, 2407.

[13] Park, J.; Kwon, S. G.; Jun, S. W.; Kim, B. H.; Hyeon, T.

ChemPhysChem **2012**, 13, 2540.

[14] Kim, B. H.; Hackett, M. J.; Park, J.; Hyeon, T. *Chem. Mater.* **2014**, 26, 59

[15] Kumara, C.; Zuo, X.; Ilavsky, J.; Chapman, K. W.; Cullen, D. A.; Dass, A. *J. Am. Chem. Soc.* **2014**, 136, 7410

[16] Kumara, C.; Zuo, X.; Cullen, D. A.; Dass, A. *ACS Nano* **2014**, 8, 6431

6. Derivation of equation

In this section, the detail derivation process of mass-to-size correlation will be shown based on Cardano's method. Eq. (1) of section 3.1 can be rearranged as Eq. (13)

$$a\boldsymbol{D}^3 + b\boldsymbol{D}^2 - \boldsymbol{M} = 0 \quad (13)$$

Cardano's method is the technique to solve third order equation by making the coefficients of second order as zero. After substitute ***D*** as *t-b/3a* for this purpose, Eq. (13) shows as follows.

$$a\left(t - \frac{b}{3a}\right)^3 + b\left(t - \frac{b}{3a}\right)^2 - \boldsymbol{M} = 0 \quad (14)$$

Eq. (14) is rearranged in the descending order of *t*.

$$t^3 - \frac{b^2}{3a^2}t + \frac{2b^3}{27a^3} - \boldsymbol{M} = 0 \quad (15)$$

To simplify the equation, ($-b^2/3a^2$) set as *p*, and ($2b^3 / 27a^3 - \boldsymbol{M}$) as *q*.

$$t^3 + pt + q = 0 \quad (16)$$

Now, another technique is introduced here. Variable t is denoted as the sum of two variables (i.e. $t = u + v$), which satisfies following condition:

$$uv = -\frac{p}{3} \quad (17)$$

Eq. (17) is rearranged with respect to u and v.

$$(u+v)^3 - 3uv(u+v) + q = 0 \quad (18)$$

We obtain eqs (19) and (20) from eqs (17) and (18)

$$u^3v^3 = -\frac{p^3}{27} \quad (19)$$

$$u^3 + v^3 = -q \quad (20)$$

Solving the simultaneous equation for u^3 and v^3, we obtained:

$$u^3 = -\frac{p}{2} + \sqrt{\frac{q^2}{4} + \frac{p^3}{27}} \quad (21)$$

$$v^3 = -\frac{p}{2} - \sqrt{\frac{q^2}{4} + \frac{p^3}{27}} \quad (22)$$

Since t is the sum of u and v by previous assumption, we get:

$$t = u + v = \sqrt[3]{-\frac{q}{2} + \sqrt{\frac{q^2}{4} + \frac{p^3}{27}}} + \sqrt[3]{-\frac{q}{2} - \sqrt{\frac{q^2}{4} + \frac{p^3}{27}}} \quad (23)$$

$$\boldsymbol{D} = t - \frac{b}{3a} = -\frac{b}{3a} + \sqrt[3]{-\frac{q}{2} + \sqrt{\frac{q^2}{4} + \frac{p^3}{27}}} + \sqrt[3]{-\frac{q}{2} - \sqrt{\frac{q^2}{4} + \frac{p^3}{27}}} \quad (24)$$

Two complex solutions are excluded because the diameter should be real number. Substituting p and q with $(-b^2/3a^2)$ and $(2b^3/27a^3 - \boldsymbol{M})$, the solution is written as follows:

$$\boldsymbol{D} = -\frac{b}{3a} + \sqrt[3]{-\frac{b^3}{27a^3} + \frac{\boldsymbol{M}}{2a} + \sqrt{-\frac{b^3\boldsymbol{M}}{27a^4} + \frac{\boldsymbol{M}^2}{4a^2}}} + \sqrt[3]{-\frac{b^3}{27a^3} + \frac{\boldsymbol{M}}{2a} - \sqrt{-\frac{b^3\boldsymbol{M}}{27a^4} + \frac{\boldsymbol{M}^2}{4a^2}}} \quad (25)$$

For conciseness, we introduce two coefficients, α and β. Finally, we get size-to-mass equation, Eq. (4) of section 3.1.

$$\boldsymbol{D} = \alpha + \sqrt[3]{\alpha^3 + \beta\boldsymbol{M} + \sqrt{2\alpha^3\beta\boldsymbol{M} + \beta^2\boldsymbol{M}^2}} + \sqrt[3]{\alpha^3 + \beta\boldsymbol{M} - \sqrt{2\alpha^3\beta\boldsymbol{M} + \beta^2\boldsymbol{M}^2}} \quad (4)$$

where

$$\alpha = -\frac{b}{3a} = -\frac{2\sigma}{\rho N_A} \quad [\mathrm{nm}] \qquad (26)$$

$$\beta = \frac{1}{2a} = \frac{3}{\rho N_A \pi} \quad [\mathrm{nm}^3/\mathrm{Da}] \qquad (27)$$

초 록

본 논문에서는 5 나노미터 이하의 은 나노입자들을 MALDI-TOF 질량 분석법을 이용하여 빠르면서도 신뢰할 수 있게 크기와 크기 분포를 결정할 수 있음을 보였다. 질량 분석 결과는 카르다노의 공식에 의해 유도된 간단한 방정식을 이용해 크기 정보로 변환될 수 있었다.

극소 은 나노입자들에 대해서 얻은 크기-질량 변환 방정식의 각 계수들은 일정하지는 않았지만 그 차이는 무시할 수 있는 수준이었다. 또한 구형 입자에서뿐만 아니라 정육면체나 팔면체 모양과 같이 이방성을 가진 입자들에 대해서도 크기-질량 변환 방정식이 이용될 수 있음을 확인했다. 이를 통해서 MALDI-TOF 질량 분석법이 크기 정보뿐 아니라 모양 정보까지도 알 수 있다는 가능성을 확인했다. 이를 통해서 MALDI-TOF 질량분석법이 나노과학에서 가치있고 다재다능한 기술로 이용될 수 있음을 보였다.

주요어 : 극소 나노입자, 은 나노입자, 말디 토프(MALDI-TOF), 질량 분석법

학 번 : 2013-20993